Nuclear Reaction Mechanisms and the Cronin Effect

G.G. Barnaföldi[1,2], G. Papp[3], P. Lévai[1] and G. Fai[4]

[1] RMKI Research Institute for Particle and Nuclear Physics,
PO Box 49, Budapest, 1525, Hungary
[2] Laboratory for Information Technology, Eötvös University
Pázmány P. 1/A, Budapest 1117, Hungary
[3] Department for Theoretical Physics, Eötvös University
Pázmány P. 1/A, Budapest 1117, Hungary
[4] Center for Nuclear Research, Department of Physics,
Kent State University, Kent, OH 44242

Presented at 10th International Conference on Nuclear Reaction Mechanism
10th June 2003, Varenna, Italy

Abstract

The influence of nuclear multiscattering and shadowing on pion spectra is investigated in pA collisions from CERN SPS to RHIC energies. The calculations are performed in a next-to-leading order (NLO) pQCD-improved parton model, including intrinsic partonic transverse momentum distributions. The nuclear modification of the pion spectra (Cronin effect) is considered at different targets in a wide energy range. Theoretical predictions are displayed for planned pA experiments at CERN SPS and recent dAu experimental results are analysed at RHIC.

1 Introduction

The Cronin effect was discovered in the energy range 20 GeV $\leq \sqrt{s} \leq$ 40 GeV at FERMILAB [1, 2, 3]. The effect is a $\sim 20-40\%$ enhancement in particle production in proton-nucleus (pA) collisions compared to scaled proton-proton (pp) ones, where the scaling factor is the *number of binary collisions*. Recent RHIC experiments at $\sqrt{s} = 200$ GeV raised the interest on this nuclear effect in nucleus-nucleus (AA) collisions. Theoretical investigations were launched to understand and reproduce the Cronin peak [4, 5, 6].

Theoretical models were based on perturbative Quantum Cromodynamics (pQCD). General problem with pQCD models, that they underestimate the experimental data by $\sim 50-100\%$ at usual scales. Changing scales could solve this problem, however larger scale causes an increase in the lower limit of applicability of pQCD calculations over the region of interest 3 GeV$\leq p_T \leq$ 6 GeV. Introducing the so called intrinsic transverse momenta (k_T), one can reproduce the experimentally measured pion (π) spectra in pp collisions within $\sim 10-20\%$. The relevant parameter of these calculations is $\langle k_T^2 \rangle$, the width of the intrinsic partonic transverse momentum distribution which depends on the c.m. energy ($\sqrt{s}$), at fix scales.

Here pion production is investigated in a wide (high-)energy range from CERN SPS up to RHIC (20 GeV $\leq \sqrt{s} \leq$ 200 GeV). Although this analysis can be revisited in case of other hadrons[6, 7], however due to the poor statistic of experimental data, in this paper we would like to reproduce only pionic data. Our calculation is performed in next-to-leading order (NLO), and compared to earlier leading order (LO) results [6].

2 Theoretical Background for pp collisions

First of all let us start with the invariant cross section for pion production in a pp collision, which can be described in the k_T-enhanced NLO pQCD-improved parton model on the basis of the factorization theorem as a convolution[8]:

$$
\begin{aligned}
E_\pi \frac{\mathrm{d}\sigma^{pp}}{\mathrm{d}^3 p_\pi} &= \frac{1}{S} \sum_{abc} \int_{VW/z_c}^{1-(1-V)/z_c} \frac{\mathrm{d}v}{v(1-v)} \int_{VW/vz_c}^{1} \frac{\mathrm{d}w}{w} \int^{1} \mathrm{d}z_c \\
&\int \mathrm{d}^2\mathbf{k}_{Ta} \int \mathrm{d}^2\mathbf{k}_{Tb}\; f_{a/p}(x_a, \mathbf{k}_{Ta}, Q^2)\, f_{b/p}(x_b, \mathbf{k}_{Tb}, Q^2) \cdot \\
&\cdot \left[\frac{\mathrm{d}\widetilde{\sigma}}{\mathrm{d}v} \delta(1-w) + \frac{\alpha_s(Q_R)}{\pi} K_{ab,c}(s, v, w, Q, Q_R, Q_F) \right] \frac{D_c^\pi(z_c, Q_F^2)}{\pi z_c^2} \; , \qquad (1)
\end{aligned}
$$

where we introduced factorised 3-dimensional parton distribution functions (PDFs),

$$
f(x, \mathbf{k}_T, Q^2) = f(x, Q^2) \cdot g(\mathbf{k}_T) \; . \qquad (2)
$$

Here, the function $f(x, Q^2)$ represents the standard 1-dimensional NLO PDF as a function of momentum fraction of the incoming parton x at factorization scale Q, $\mathrm{d}\widetilde{\sigma}/\mathrm{d}v$ represents the Born cross section of the partonic subprocess $ab \to cd$, $K_{ab,c}(s, v, w, Q, Q_R, Q_F)$ is the corresponding higher order correction term, and the fragmentation function (FF), $D_c^\pi(z_c, Q_F^2)$, gives the probability for parton c to fragment into a pion with momentum fraction z_c at fragmentation scale Q_F. We use the conventional proton level (S, V, W) and parton level (s, v, w) kinematical variables of NLO calculations (see Ref.s [8, 9, 10]).

In this analysis we consider fixed scales: the factorization and the renormalization scales are connected to the momentum of the intermediate jet, $Q = Q_R = \kappa \cdot p_q$ (where $p_q = p_T/z_c$), while the fragmentation scale is connected to the final hadron momentum, $Q_F = \kappa \cdot p_T$. The value of κ is $\sim \mathcal{O}(1)$.

For our NLO calculations we are using a 3-dimensional PDF which is a product of the standard PDF (at its Q scale) and a 2-dimensional initial transverse-momentum distribution, $g(\mathbf{k}_T)$ of partons containing its "intrinsic k_T" parameter as in Refs. [6, 8, 4, 5]. We demonstrated the success of such a treatment at LO level in Ref. [6], and a K_{jet}-based NLO calculations in [11, 12]. In our phenomenological approach the transverse-momentum distribution is described by a Gaussian,

$$
g(\mathbf{k}_T) = \frac{1}{\pi \langle k_T^2 \rangle} e^{-k_T^2/\langle k_T^2 \rangle} \; . \qquad (3)
$$

Here, $\langle k_T^2 \rangle$ is the 2-dimensional width of the k_T distribution and it is related to the magnitude of the average transverse momentum of a parton as $\langle k_T^2 \rangle = 4\langle k_T \rangle^2/\pi$.

In present article we use the LO GRV[13], and the NLO MRST(cg)[14] PDFs. For FF we apply most recent KKP parameterizations [15], both in LO and NLO cases. These PDF and FF sets can be applied down to very small scales ($Q^2 \approx 1.25$ GeV^2), thus we have got results at relatively small transverse momenta, $p_T \geq 2$ GeV at our fix scales. The details of the NLO calculations can be found in Ref. [8]

In our earlier work[6] we determined the p_T-independent intristic-k_T values for the 3 GeV $\leq p_T \leq$ 6 GeV momentum window and investigated their dependence on c.m. energy at fixed scales[11]. We found that the reproduction of the Cronin effect requires $\langle k_T^2 \rangle \approx 2$ GeV^2. The di-jet production data at ISR energies yield a similar value for $\langle k_T^2 \rangle$ [16]. Recent measurements of jet-jet correlations in pp collision at RHIC energies[17, 18] can clarify the properties of the transverse component of the PDFs.

Our description of pion production in pp collision can be extended for pA and AA collisions.

3 Nuclear Effects in pA and AA Collisions

Proton-nucleus and nucleus-nucleus collisions can be described by including collision geometry, saturation in nucleon-nucleon (NN) collision number, and shadowing inside the nucleus. In the frame of Glauber picture, the cross section of pion production in nucleus-nucleus collision can be written as an integral over impact parameter b:

$$E_\pi \frac{\mathrm{d}\sigma_\pi^{AA'}}{\mathrm{d}^3p} = \int \mathrm{d}^2b\,\mathrm{d}^2r\; t_A(r)\; t_{A'}(|\mathbf{b}-\mathbf{r}|) \cdot E_\pi \frac{\mathrm{d}\sigma_\pi^{pp}(\langle k_T^2\rangle_{pA}, \langle k_T^2\rangle_{pA'})}{\mathrm{d}^3p} \ , \tag{4}$$

where pp cross section on the right hand side represents the cross section from eq. (1), but with an increased widths compared to the original transverse-momentum distributions (3) in pp collisions, as a consequence of nuclear multiscattering (see eq. (5)). Here $t_A(b) = \int \mathrm{d}z\, \rho_A(b,z)$ is the nuclear thickness function (in terms of the density distribution of nucleus A, ρ_A), normalized as $\int \mathrm{d}^2b\, t_A(b) = A$. For small size nucleus we used sharp sphere approximation, while for larger nuclei Wood-Saxon formula were applied.

The initial state broadening of the incoming parton's distribution function is accounted for by an increase in the width of the Gaussian parton transverse momentum distribution in eq. (3):

$$\langle k_T^2\rangle_{pA} = \langle k_T^2\rangle_{pp} + C \cdot h_{pA}(b) \ . \tag{5}$$

Here, $\langle k_T^2\rangle_{pp}$ is the width of the transverse momentum distribution of partons in pp collisions, $h_{pA}(b)$ describes the number of *effective* NN collisions at impact parameter b, which impart an average transverse momentum squared C. The effectivity function $h_{pA}(b)$ can be written in terms of the number of collisions suffered by the incoming proton in the target nucleus, $\nu_A(b) = \sigma_{NN} t_A(b)$, where σ_{NN} is the inelastic NN cross section:

$$h_{pA}(b) = \begin{cases} \nu_A(b) - 1 & \nu_A(b) < \nu_m \\ \nu_m - 1 & \text{otherwise} \end{cases} \ . \tag{6}$$

The value $\nu_m = \infty$ corresponds to the case where all possible semihard collisions contribute to the broadening. We have found that for realistic nuclei the maximum number of semihard collisions is $3 \le \nu_m \le 4$.

The determination of the factor C and of $\nu_A(b)$ is in progress in a systematic analysis in NLO [19]. Our preliminary results confirm the findings of Ref. [6], where the systematic analysis of pA reactions was performed in LO and the characteristics of the Cronin effect were determined at LO level. Following Ref. [6], we assume that only a limited number of semi-hard collisions (with $\nu_m = 4$) contributes to the broadening, average momentum squared imparted per collision is $C = 0.4\ \mathrm{GeV}^2$.

Furthermore, the PDFs are modified in the nuclear environment by the "shadowing" effect[20, 21, 22]. This effect and isospin asymmetry are taken into account on average using a scale independent parameterization of the shadowing function $S_{a/A}(x)$ adopted from Ref. [4]:

$$f_{a/A}(x,Q^2) = S_{a/A}(x) \left[\frac{Z}{A} f_{a/p}(x,Q^2) + \left(1 - \frac{Z}{A}\right) f_{a/n}(x,Q^2)\right] \ , \tag{7}$$

where $f_{a/n}(x,Q^2)$ is the PDF for the neutron and Z is the number of protons. In the present work, we display results obtained with the EKS parameterization [21], and with the updated HIJING parameterization[20]. The former has an antishadowing feature, while the later incorporates different quark and gluon shadowing, and has an impact-parameter dependent and an impact-parameter independent version. The impact-parameter dependence is taken into account by a term $\propto (1 - b^2/R_A^2)$, which re-weighs the shadowing effect inside the nucleus.

We note, that for the deuteron (d), one could use a simple superposition of a pAu and a nAu collision, or a distribution for the nucleons inside the deuteron. For a first orientation we follow Ref. [23, 24] in this regard, and apply a hard-sphere approximation for the deuteron with $A = 2$ taking no nuclear effects for the deuteron.

4 Results on the Cronin Effect

Including these effects one can calculate the invariant cross section for an AA' collision. Thus, introducing the nuclear modification factor $R_{AA'}$, as

$$R^{\pi}_{AA'} = \frac{\mathrm{d}\sigma^{AA'}_{\pi}/\mathrm{d}^3p \ (\text{“included nuclear effects”})}{\mathrm{d}\sigma^{AA'}_{\pi}/\mathrm{d}^3p \ (\text{“no nuclear effect”})} \ , \tag{8}$$

nuclear effects can be investigated clearly and efficiently, on a linear scale.

Following[1, 2] for the nuclear modification factor, in Figure 1, we present the Cronin effect as a ratio of pW to pBe collisions ($R_{W/Be}$). This “type” of nuclear modification factor, is principally insensitive to the shadowing at CERN SPS energies. We compared experimental data[1, 2, 3], with theoretical calculations at $\sqrt{s} = 19.4$, 23.8, 27.4 and 38.8 AGeV c.m. energies. In all calculation we choose $\langle k_T^2 \rangle \approx 2$ GeV^2, $\nu_m = 4$ and $C_{sat} = 0.4$ GeV^2 for all A, while the scale was fixed as $\kappa = 1/2$ in case of LO calculations (*dotted lines*). In NLO case the scales are chosen as $\kappa = 2/3$. It seems there is no difference (within $\sim 5\%$) between curves with no shadowing (*solid lines*) and with the updated HIJING b-independent (*dashed*) or b-dependent (*dash-dotted*) lines.

Figure 2 presents the dependence of R_{pA} (*left panel*) and $R_{A/Be}$ (*right panel*) on different targets $A \in \{\ ^9Be, \ ^{32}S, \ ^{44}Ti, \ ^{98}In$ and $^{197}Au\ \}$ at CERN SPS energies in NLO calculations at $E_{beam} = 158$ AGeV, with $\langle k_T^2 \rangle = 1.9$ GeV^2 . We present our results with EKS shadowing (*dotted lines*), the b-independent, and the b-dependent updated HIJING shadowings (*solid lines*). The b-independent and b-dependent updated HIJING cases are coincide within errors.

In our model the position of Cronin peak does not depend explicitely on the c.m. energy, however, depends on the value of $\langle k_T^2 \rangle$. With the above scale choices the peak is appears at $p_T \approx 4$ GeV. Furthermore, the height of the peak depends on the A via $C \cdot h_{pA}(b)$ term in eq. 5. (see Fig. 1). In the energy range 20 GeV $\leq \sqrt{s} \leq 40$ GeV shadowing effects are generally small. Thus, the influence of the different shadowings on the Cronin effect are negligible, especially in minimum bias cases (see Fig. 2).

In Figure 3 we display our NLO results for the nuclear modification factor in dAu collision for b-independent (*solid line*) and b-dependent (*dashed line*) shadowing parameterizations from the updated HIJING shadowing using parameters ($\sqrt{s} = 200$ AGeV, $\langle k_T^2 \rangle = 2.5$ GeV^2, $\kappa = 4/3$). In spite of the very different impact parameter dependence of R_{dAu} the minimum bias results are very close to each other. This is because many details are averaged out in minimum bias data, and the final result is no longer sensitive to the b-dependence of shadowing. As we can see on Fig. 3 the theoretical results reproduce quite well the minimum bias experimental data on π^0 from PHENIX[25]. In minimum bias case we do not see a strong Cronin peak. However, a reasonable Cronin peak will appear in different centrality bins.

Figure 4 summarizes our results on the impact-parameter (b) dependence of the Cronin effect in dAu collision [24]. The nuclear modification factor, $R_{dAu}(b)$, is presented with updated HIJING shadowing. The *left* column shows the b-independent cases, while the *right* column displays the b-dependent ones.

Applying b-independent shadowing for central collisions (*left upper panel*) the curves overlap, since in these bins, the target matter is approximately constant from the point of view of multiscattering and shadowing. In more peripheral cases (*left lower panel*), shadowing starts to dominate, $R_{dAu}(b)$ is decreasing from bin to bin. The b-independent shadowing suppresses $R_{dAu}(b)$ under 1.

In case of b-dependent shadowing at central bins (*right upper panel*) Cronin effect wins against suppression. At peripheral bins (*right lower panel*) – where Cronin effect begin to vanish and shadowing suppression working also –, the nuclear modification factor becomes unity.

5 Summary

We investigated pp and pA experimental data on pion production with our k_T-augmented pQCD parton model at NLO level in the c.m. energy window 20 AGeV $\leq \sqrt{s} \leq$ 200 AGeV. In the lower limit of this energy range ($\sqrt{s} \leq$ 40 AGeV), the pion p_T-spectra is not sensitive to the applied shadowing mechanism, because shadowing is close to be negligible ($\sim$ 5%) in this kinematical region. However the multiscattering strongly influences this spectra and dominates every deviation of pA collision from superimposed nucleon-nucleon collisions We determined the most important parameters of the parton model from existing experimental data and we predicted the Cronin effect in pA collisions at CERN SPS energy (E_{beam} = 158 AGeV). Considering different targets (^9Be, ^{32}S, ^{44}Ti, ^{98}In and ^{197}Au) we obtained an increasing multiscattering effect with increasing size of the target nucleus, while the position of the Cronin peak did not change.

Our analysis was repeated at RHIC energy ($\sqrt{s}$ = 200 AGeV). Here the shadowing effect is much larger, thus the differences between the competing shadowing models are emphasized. Applying b-dependent shadowing description for the dAu collision the centrality dependence of the Cronin effect generates an unusual structure in the nuclear modification factor, which can be measured experimentally. In this way we can distinguish between different shadowing models from the data. However minimum bias calculations yields similar results for different shadowing models. Using our model we successfully reproduced the measured nuclear modification factor for π^0 in the dAu collision.

Acknowledgments

This work was supported in part by Hungarian grants: T034842, T043455, T043514; U.S. DOE grant: DE-FG02-86ER40251, and NSF grant: INT-0000211 Supercomputer time provided by BCPL in Norway and the EC – Access to Research Infrastructure action of the Improving Human Potential Programme is gratefully acknowledged.

References

[1] J.W. Cronin et *al.* (CP Coll.), Phys. Rev. **D11**, 3105 (1975);

[2] D. Antreasyan et *al.* (CP Coll.), Phys. Rev. **D19**, 764 (1979);

[3] D.E. Jaffe et *al.* (E605 Coll.), Phys. Rev. **D40**, 2777 (1989);

[4] X.N. Wang, Phys. Rev. **C61**, 064910 (2001);

[5] C.Y. Wong and H. Wang, Phys. Rev. **C58,** 376 (1998);

[6] Y. Zhang, G. Fai, G. Papp, G.G. Barnaföldi, and P. Lévai, Phys. Rev. **C65**, 034903 (2002);

[7] X. Zhang and G. Fai, `hep-ph/0306227`;

[8] G. Papp, G.G. Barnaföldi, P. Lévai, and G. Fai, `hep-ph/0212249`;

[9] F. Aversa, P. Chiappetta, M. Greco, and J.Ph. Guillet, Nucl. Phys. **B327**, 105 (1989);

[10] P. Aurenche, M. Fontannaz, J.Ph. Guillet, B. Kniehl, E. Pilon, and M. Werlen, Eur. Phys. J. **C9**, 107 (1999);
P. Aurenche, M. Fontannaz, J.Ph. Guillet, B. Kniehl, and M. Werlen, Eur. Phys. J. **C13**, 347 (2001);

[11] G.G. Barnaföldi, P. Lévai, G. Papp, G. Fai, and Y. Zhang, (in print) APH NS Heavy Ion Phys. **18** (2003), `nucl-th/0206006`;

[12] G.G. Barnaföldi, P. Lévai, G. Papp, G. Fai, and Y. Zhang, (in print) Proc. of ISMD '02 World Sci. (2003), `nucl-th/0212111`;

[13] M. Gluck, E. Reya and A. Vogt, Z. Phys. **C67**, 433 (1995);

[14] A.D. Martin, R.G. Roberts, W.J. Stirling, and R.S. Thorne, Eur. Phys. J. **C23**, 73 (2002);

[15] B.A. Kniehl, G. Kramer and B. Pötter, Nucl. Phys. **B597**, 337 (2001), `hep-ph/0011155`;

[16] A.L.S. Angelis, *et al.* (CCOR Coll.), Phys. Lett. **B97**, 163 (1980);

[17] C. Adler *et al.* (STAR Coll.), Phys. Rev. Lett. **90**, 082302 (2003);
D. Hardtke *et al.* (STAR Coll.), Nucl. Phys. **A715**, 801c (2003);

[18] J. Rak *et al.* (PHENIX Coll.), `nucl-ex/0306031` ;

[19] G.G. Barnaföldi, P. Lévai, G. Papp, and G. Fai, (in preparation);

[20] S.J. Li and X.N. Wang, Phys. Lett. **B527**, 85 (2002);

[21] K.J. Eskola, V.J. Kolhinen and C.A. Salgado, Eur. Phys. J. **C9**, 61 (1999);

[22] M. Hirai, S. Kumano and M. Miyama, Phys. Rev. **D64**, 034003 (2001);

[23] I. Vitev, Phys. Lett. **B562**, 36 (2003);

[24] P. Lévai, G. Papp, G.G. Barnaföldi and G. Fai, `nucl-th/0306019`;

[25] S.S. Adler *et al.* (PHENIX Coll.), `nucl-th/0306021`;

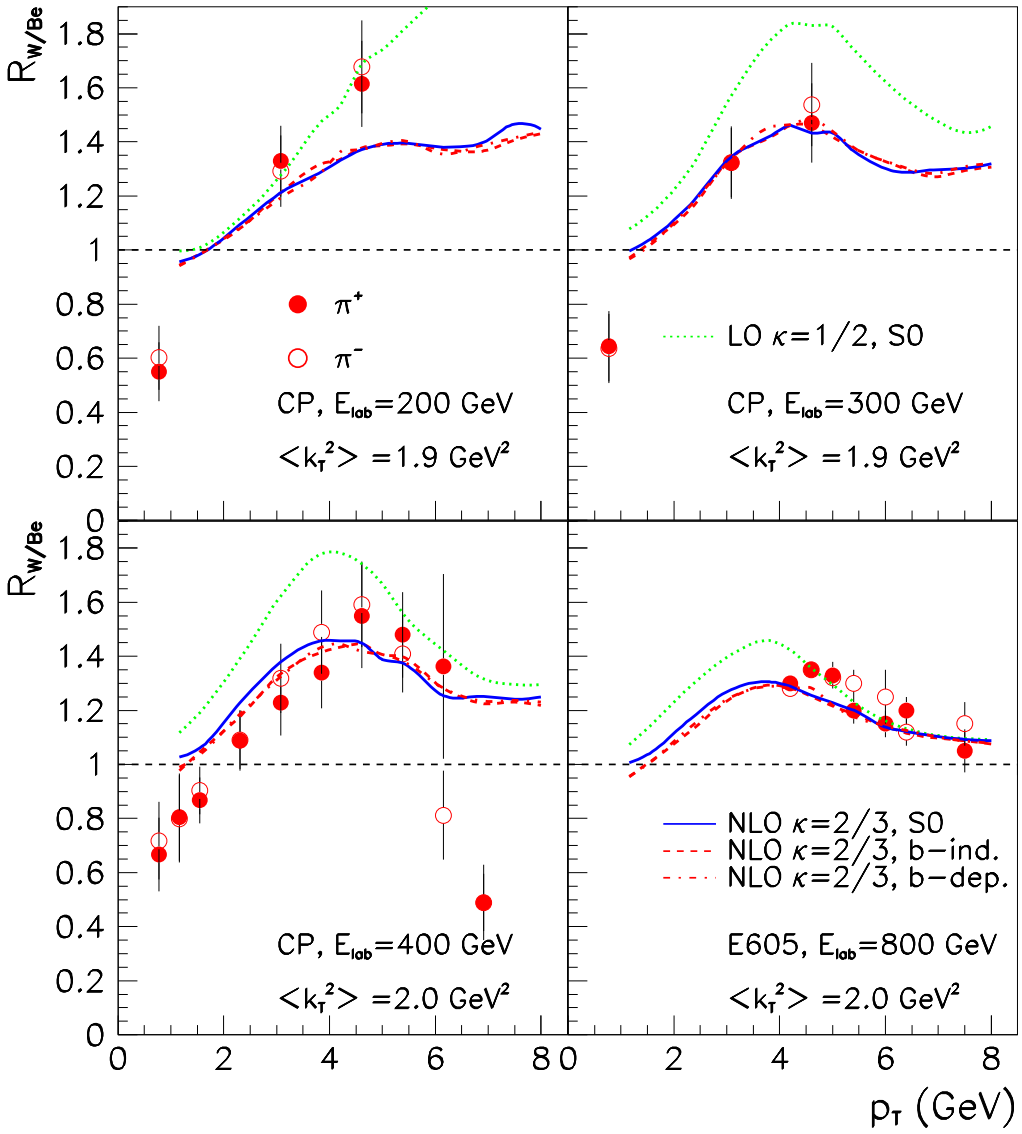

FIG. 1. Cronin effect on $R_{W/Be}$ nuclear modification factor at CERN SPS energies, from $\sqrt{s} =$ 19.3 AGeV up to 38.8 AGeV compared to experimental data[1, 2, 3]. Curves are in LO with *dotted*, in NLO with no shadowing *(S0)* with *solid*, and in NLO with updated HIJING shadowing[20] both in b-independent *dashed* and b-dependent *dash-dotted lines* cases. The later two are not different within errors. All calculations were carried out using $\nu_m = 4$, $C_{sat} = 0.4$ GeV^2, and with $\langle k_T^2 \rangle$ shown. We applied scales: $\kappa = 1/2$ in LO and $\kappa = 2/3$ in NLO.

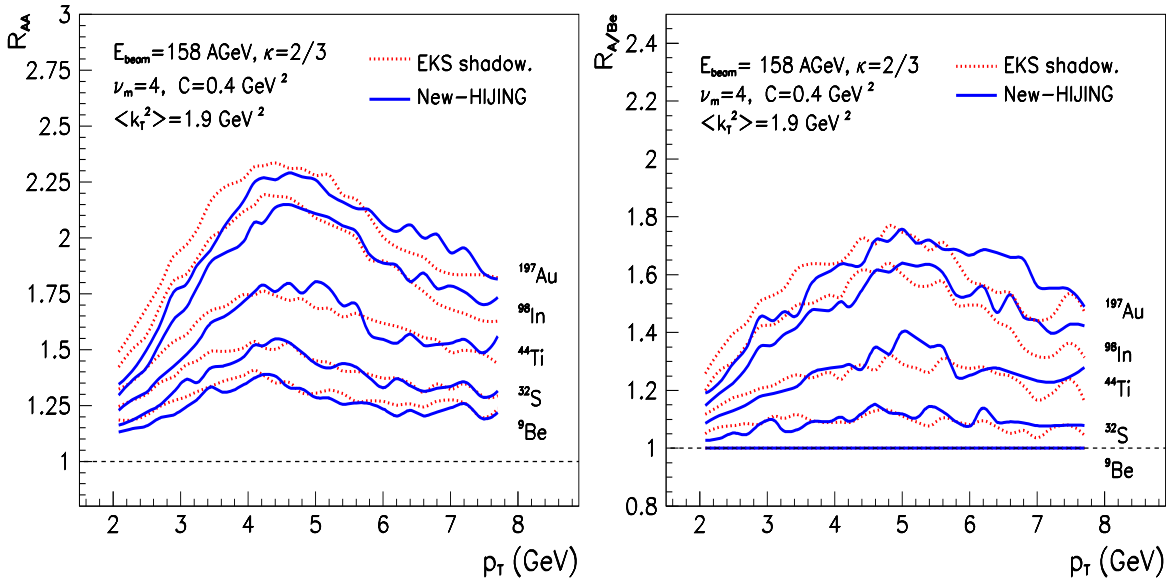

FIG. 2. Dependence of $R_{AA'}(p_T)$ (*left panel*) and $R_{A/Be}(p_T)$ (*right panel*) on different A targets ($A \in \{^9Be,\ ^{32}S,\ ^{44}Ti,\ ^{98}In$ and $^{197}Au\}$) at CERN SPS energies. We presented our results on three types of shadowing: EKS by Eskola et *al.*[21] (*dotted lines*), and new HIJING[20] shadowing (*solid lines*). The NLO calculations were carried out at $E_{beam} = 158$ AGeV, $\langle k_T^2 \rangle = 1.9$ GeV^2 and at $\kappa = 2/3$.

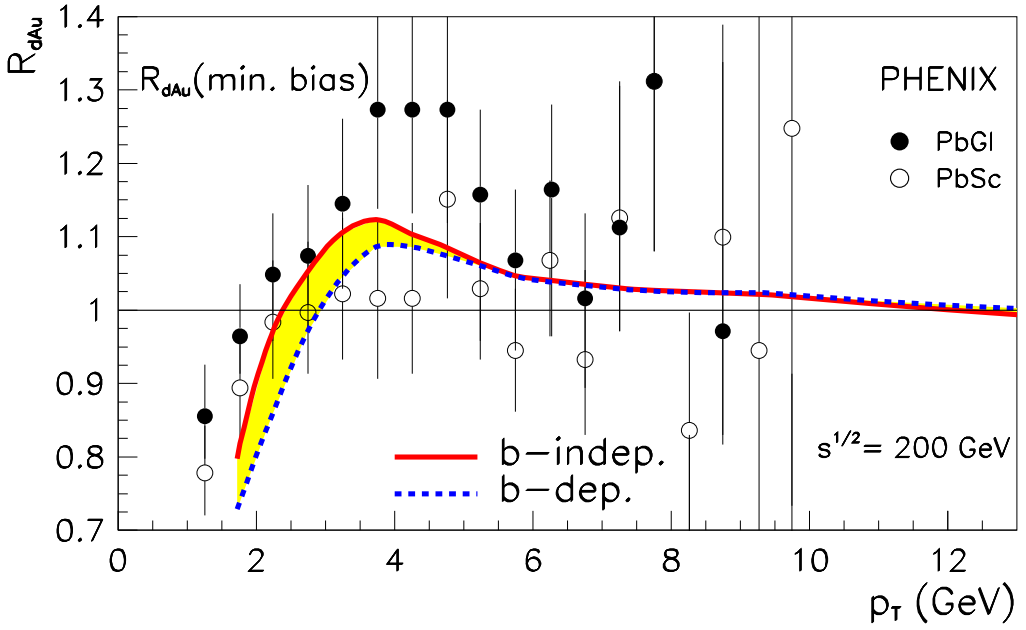

FIG. 3. The nuclear modification factor R_{dAu} for minimum bias dAu collisions obtained from our NLO calculation in case of updated HIJING b-independent, (*solid line*) and b-dependent shadowing (*dashed line*). Theoretical calculations are compared to two different experimantal sets PbGl (*dots*) and PbSc (*open circles*) at PHENIX [25].

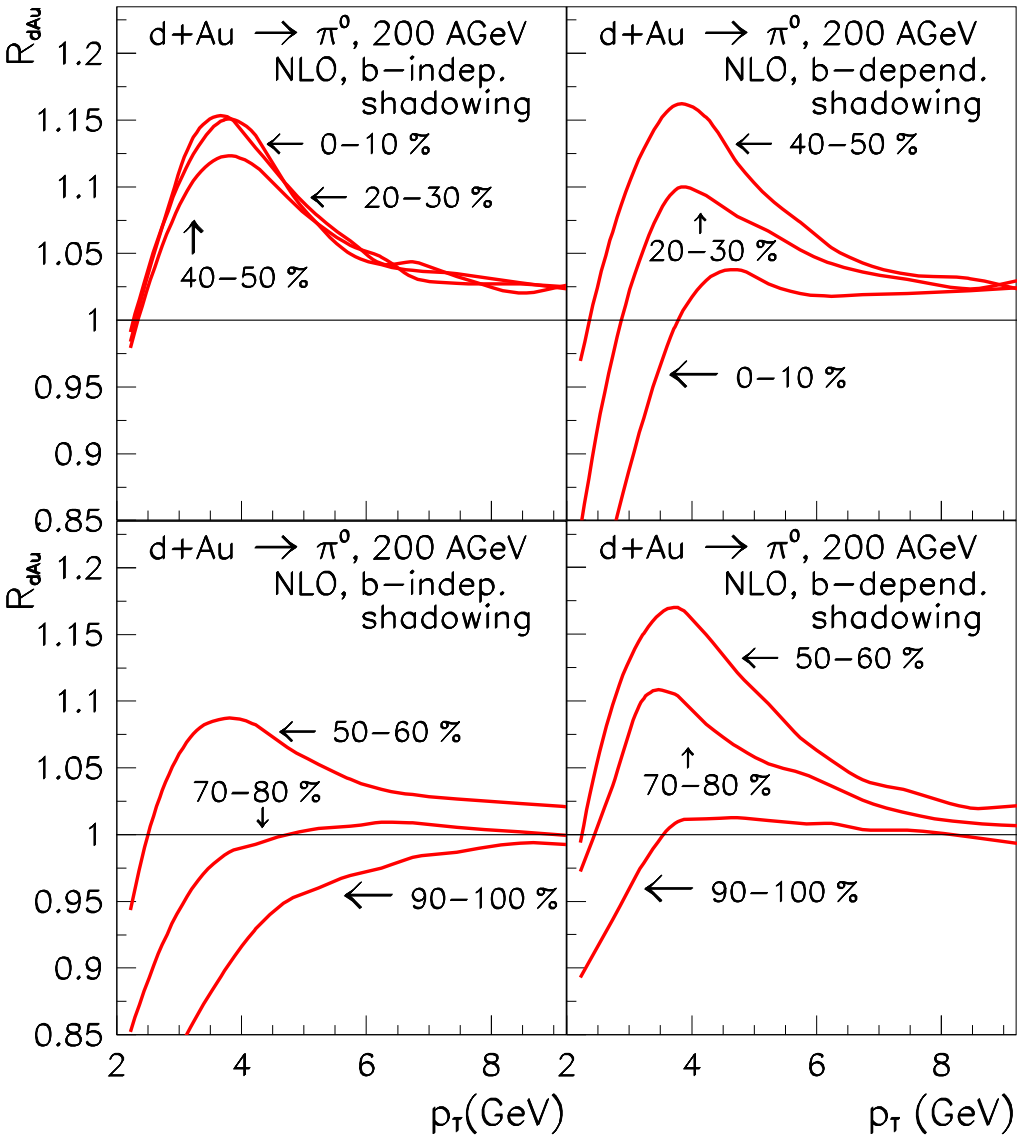

FIG. 4. The impact parameter (b) dependence of the nuclear modification factor $R_{dAu}(b)$ with b-independent shadowing (*right column*) and with b-dependent shadowing (*left column*). The lines correspond to different centrality bins. The 3 "central" curves (0-50%) are shown in the *upper panels*, and the remaining 3 "peripheral" cases (50-100%) can be seen in the *lower panels*.